

Study of the Photo-Response of Doped GaAs with Aging

Samuel Zambrano Rojas ^{1,*} and Gerardo Fonthal ^{2,*} ¹ Grupo de Investigacion en Fisica del Estado Solido, Universidad de la Guajira, Rihoacha 440007, Colombia² Instituto Interdisciplinario de las Ciencias, Universidad del Quindio, Armenia 630001, Colombia

* Correspondence: szambrano@uniguajira.edu.co (S.Z.R.); gfonthal@uniquindio.edu.co (G.F.)

Abstract: The aging of semiconductor materials is a topic of current interest. We studied the photo-response of epitaxial samples of GaAs doped with Ge and Sn up to 1×10^{19} atoms cm^{-3} . These samples were stored in a dry and dark environment for 26 years. We realized photoluminescence measurements at different temperatures and photoreflectance spectra at 300 K in three periods: 1995, 2001 and 2021. We found that environmental oxygen formed defects in GaAs, leaving lattice vacancies that provoked changes in the optical photo-response. In addition, we found that the vacancy concentrations could be as large as 5×10^{17} atoms cm^{-3} over the 26 years. In this work, we demonstrate that the aging of semiconductor materials occurs even when they are not used within a functioning circuit, with the changes being greater when the material is not doped. Knowing about the aging of materials is important for the industry, particularly for the semiconductor industry, because aging-induced deterioration influences prices and guarantees.

Keywords: aging; optical response; doped GaAs; defects

1. Introduction

Users of semiconductor materials assume that they are inert materials that do not change over time. However, it is useful to check whether or not their physical properties have been affected over time since they were produced. The warranty duration of devices, for which climatic conditions play an important role, is decided based on the efficiency of operation. The aging process can affect the structural and optical properties of aging-sensitive materials. Changes in the structural properties of the material can be caused by phase transformations and the deformation or damage of the surface over time. These structural changes will cause changes in optical, electrical, thermal and other responses. Thus, the classification of materials can be carried out in three differentiated parts based on their response to aging: short, long and very-long material sensitivity to aging. In many scientific research labs, experiments are performed with semiconductor wafers, whether purchased or manufactured. If the experiment is non-destructive, those samples are stored on shelves under ambient conditions for several years before another experiment. However, it is often not taken into account that there is a slow internal dynamic within the solid material that can alter its physical properties over time. On the other hand, the devices manufactured in companies are encapsulated to protect them from environmental conditions, but the aging process continues over time. Aging is one of these types of degradation that can affect the performance of devices designed with these materials [1,2]. In the last decades, some theoretical and experimental studies have shown a growing interest in the analysis of the effects of aging and the rate of degradation in semiconductor materials [3,4] and luminescent ceramics [5]. These studies are carried out with the purpose of understanding, simulating and mitigating their impact during the design phase of devices for technological and industrial applications, as described by Kim and his group [6]. Semiconductor degradation is due to the accumulation of defects in the crystalline structure of the material. Several studies have explored the aging of semiconductor materials. Kumara et al. [7] carried out an investigation on the optical response of doped and undoped ZrO_2 epitaxial



Citation: Zambrano Rojas, S.; Fonthal, G. Study of the Photo-Response of Doped GaAs with Aging. *Appl. Sci.* **2024**, *14*, 3806. <https://doi.org/10.3390/app14093806>

Academic Editor: Michael (Misha) Sumetsky

Received: 27 September 2023

Revised: 18 October 2023

Accepted: 25 October 2023

Published: 29 April 2024



Copyright: © 2024 by the authors. Licensee MDPI, Basel, Switzerland. This article is an open access article distributed under the terms and conditions of the Creative Commons Attribution (CC BY) license (<https://creativecommons.org/licenses/by/4.0/>).

films and observed a decrease in the energy band as the aging time increased. On the other hand, Song et al. [8] applied different experimental techniques to analyze failures in high-power semiconductor lasers subjected to accelerated aging. All these works show that the study of the aging of semiconductor materials is still a current topic and some techniques have even been used to accelerate the aging process for analysis in the laboratory [9–11]. In particular, Neuhod et al. [12] studied the formation of monodeflects in GaAs when exposed to high-energy proton irradiation. GaAs is a widely studied semiconductor material with multiple applications in electronic and optoelectronic devices. We selected GaAs for this study because it is a widely characterized semiconductor material, which allows comparisons to be made with our measurements. In this work, we study the aging dynamics through optical techniques such as photoluminescence (PL) and photoreflectance (PR), during three periods of time over 26 years on doped and undoped GaAs epitaxial films that are exposed to the environment.

2. Materials and Methods

In 1995, 10 μm thick GaAs:Sn and GaAs:Ge films were grown on a GaAs substrate oriented in the (100) direction by Liquid Phase Epitaxy at a temperature of 800 $^{\circ}\text{C}$. The precursor materials used to grow the film were Ga(7N), Ge(5N) and Sn(5N), including the purity in parentheses, and also GaAs to obtain As [13]. Through this method, the resulting films contained native defects such as V_{As} and interstitial Ga due to excessive Ga [14]. To facilitate crystalline ordering and avoid deep defects or traps, thermal annealing was performed at 620 $^{\circ}\text{C}$ for 4 h in an H_2 environment. The Ge concentrations ranged from 1×10^{16} atoms cm^{-3} to 1×10^{19} atoms cm^{-3} and the Sn concentrations ranged from 1×10^{17} atoms cm^{-3} to 2×10^{18} atoms cm^{-3} . The impurity concentrations were measured by the capacitance-voltage method. A C-V Plotter Princeton Applied Research Mod 410 was used to obtain the capacitance (C) at different applied voltages (V). Through the $1/C^2$ vs. V graph, the slope of the line was measured, which is proportional to the inverse of the concentration N of the impurities. We have assumed that all impurities are ionized at room temperature due to their low ionization energies.

In this study, PL and PR were measured in those samples. Subsequently, all GaAs epitaxial samples were stored in closed cabinets with the following environmental characteristics: atmospheric pressure of 1017 hPa, average temperature of 24 $^{\circ}\text{C}$, relative humidity of 76% and darkness. In 2001, Fonthal [14] re-measured PL at different temperatures and PR at 300 K and stored the samples in the same environment conditions for another 20 years. In 2021, again, we took the PL and PR spectra of these samples.

The PL system in this work used an external excitation source, a laser with a wavelength of 488 nm focused on the sample by a cylindrical lens. A convergent lens in the entrance slit of a Horiba FHR1000 spectrophotometer focused the light emission from the sample under study. To remove the Rayleigh radiation reflected by the sample, an LP'488 filter was located in the entrance slit. The spectrophotometer has a diffraction grating of 1800 lines per millimeter, a focal distance of 100 cm and a spectral resolution of 0.010. A CCD camera with thermo-electric cooling, was used as a photodetector. The samples were placed inside a cold finger cooled through a closed circuit of liquid He. The temperature was measured through a carbon resistance. Measurements were made between 13 K and 300 K. The PR spectra were recorded by using a modulation source, a He–Ne laser with a wavelength of 488 nm, cut by a mechanical chopper attached to a lock-in amplifier. The radiation probe from a quartz-tungsten-halogen lamp was passed through a monochromator. The detector used in this technique was a PbS photopin. Measurements were made at 300 K.

3. Results and Discussion

PL is a suitable technique for studying radiative electronic transitions. For semiconductors, these transitions are made around the energy gap (E_g), which separates the valence band and the conduction band. If the concentration of the impurities does not exceed the

Mott limit, the Fermi level is within the energy gap, separating the states occupied by electrons from those unoccupied. The impurity states are placed within that energy gap close to the conduction band if the impurity is a donor type, and close to the valence band if the impurity is an acceptor type. When there are defects in the crystal lattice, they produce electron traps which are located very deep in energy within the energy gap. Based on the above understanding and by analyzing the photoluminescence spectra of the semiconductors, the highest energy transitions correspond to the transition of the conduction band to the valence band (B-B). The excitonic transitions (X) will be in lower energy and involve the interaction of an electron from the conduction band, but that has been attracted by a hole in the valence band. In the semiconductor industry, the PL width of the excitonic peak is used to test the crystalline quality of the grown solid. A narrower excitonic peak indicates better crystalline quality of the material. At even lower energy, the transitions involving impurity states either from a band to an impurity state or between two impurity states. The least energetic, that is, the furthest from the B-B transition, will be the transitions that involve defect states.

In Figure 1, we show in black the photoluminescence results for the undoped GaAs sample used by Torres [13] in 1995. In 2001, Fonthal [14] measured the PL spectrum in that same sample, which was stored for 6 years in the environmental conditions described above. Fonthal's spectrum is represented in red. This same sample was employed in 2021 for this study and its spectrum is illustrated in blue. It is evident that there has been a change in the optical response of the undoped GaAs sample over time due to aging, at least within the laser penetration length of the PL technique. For a better understanding of the PL spectra in Figure 1, we have superimposed an orange line at 1.375 eV to separate two spectral zones. The highest energy zone corresponds to the transitions that involve the energy bands and impurities. The zone below 1.375 eV is the zone corresponding to deep trap transitions due to defects. In the impurity zone, excitonic peaks are distinguished near the E_g at 1.424 eV and a second peak around 1.385 eV that corresponds to the donor-acceptor transition of shallow impurities. It can be distinguished that in the blue spectral curve, the excitonic peak broadens and shifts towards higher energies compared to other lower aging spectra. This is due to the deterioration of the crystalline quality of the material over time. On the other hand, the zone below 1.375 eV shows a broad peak that corresponds to the transitions involving deep defects. We have called this peak DT for the spectrum taken in 1995, DF for the one taken in 2001 and DO for the one measured in 2021. In this second area, it can be observed that the peak of deep traps moves towards lower energy values, broadens and increases in intensity with respect to the excitonic peak as the sample ages. This is due to the increasing concentration of defects in the samples as the years go by.

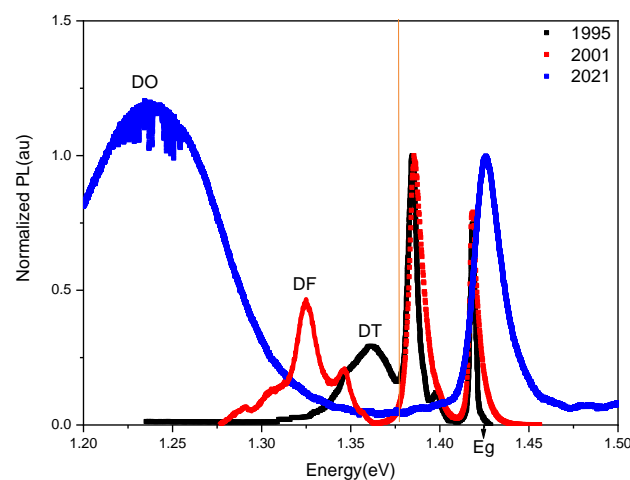


Figure 1. Normalized photoluminescence spectra obtained using a 488 nm laser at a temperature of 300 K, taken on different dates for an undoped GaAs sample. The spectrum in black is taken from reference [13] and the one in red is taken from [14].

In Figure 1, we can observe that in the black spectrum obtained by Torres, there is a defects band (DT) centered at 1.356 eV, just after the sample was grown. This band corresponds to what is called a native defect, which has been reported by several authors for the case of GaAs [15,16] as $V_{As}-I_{As}$, where the letter I represents impurities. The formation of Ga and As oxides slowly over many years due to the presence of oxygen, adding defects to the surface, as suggested by Birey and Site [17] and Bunea and Dunham [18]. In the same, it also shows the red PL spectrum obtained by Fonthal six years later, and one can see that the defect zone (DF) has expanded and shifted towards lower energies, now centering at 1.324 eV. This means that new defects have been formed in greater quantity. For this work, we measured the blue spectrum of PL 26 years after the undoped GaAs sample was grown. The defect peak (DO) has shifted towards 1.244 eV and has grown significantly and broadened.

In Figure 2, we show the PL spectra for different undoped and doped GaAs samples at 13 K temperature taken in 2021. The influence of doping in 26-year-old samples is clear. The undoped sample in magenta shows the maximum peak in the defect zone at 1.335 eV. It can be distinguished in the spectrum at 13 K of this sample that the excitonic peak is higher than that of defects, contrary to the blue spectrum at 300 K in Figure 1. The temperature destroys the electron-hole bond of the exciton.

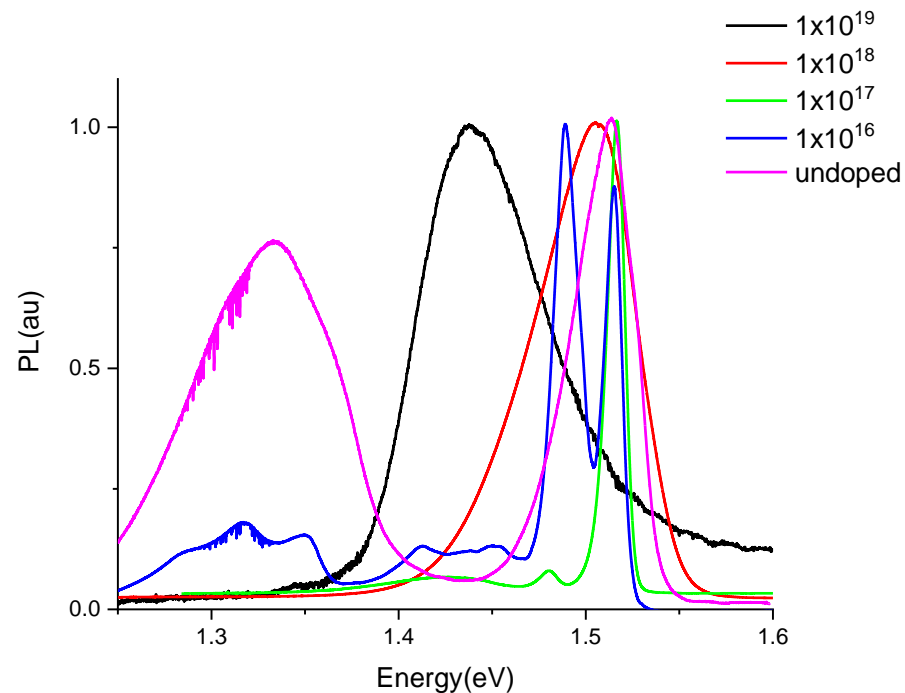


Figure 2. Photoluminescence spectra for different doped GaAs samples at 13 K temperature taken in 2021.

We already explained in another article [19] that this peak of defects is due to the formation of vacancies, especially for the As vacancies. The blue spectrum in Figure 2, which corresponds to the sample doped with 1×10^{16} atoms cm^{-3} , shows this same defect peak at 1.324 eV, but is more diminished with structure. For the green line of the 1×10^{17} atoms cm^{-3} sample, that peak is even lower than 1×10^{16} atoms cm^{-3} and then this peak disappears for a higher doping level. The excitonic peak is close to the bandgap at 1.512 eV in the blue spectrum with 1×10^{16} atoms cm^{-3} . In addition to the excitonic peak near the energy gap, other peaks appear at 1.49, 1.45 and 1.41 eV, corresponding to the transitions that involve the bands and/or impurity levels. These latter peaks widen with increasing concentration of the impurities, until they overlap within a single peak for higher concentrations, as seen for the red and black spectra in Figure 2. In the undoped GaAs, this peak is not resolved, indicating a low crystallinity of the sample. As the doping in

the semiconductor is increased, the excitonic peak resolves, i.e., the crystallinity improves. This is because the impurities occupy Ga sites and As sites and do not allow the formation of vacancies of those elements, as was also shown in reference [19]. With the increase in impurity, crystallinity is once again lost, due to the substitutional defects that generate shallow energy levels and not deep ones such as vacancies.

Figure 3 shows the PL spectra of the defect zone for the GaAs:Sn 1×10^{17} atoms cm^{-3} sample taken in 2001 and 2021 at low temperatures.

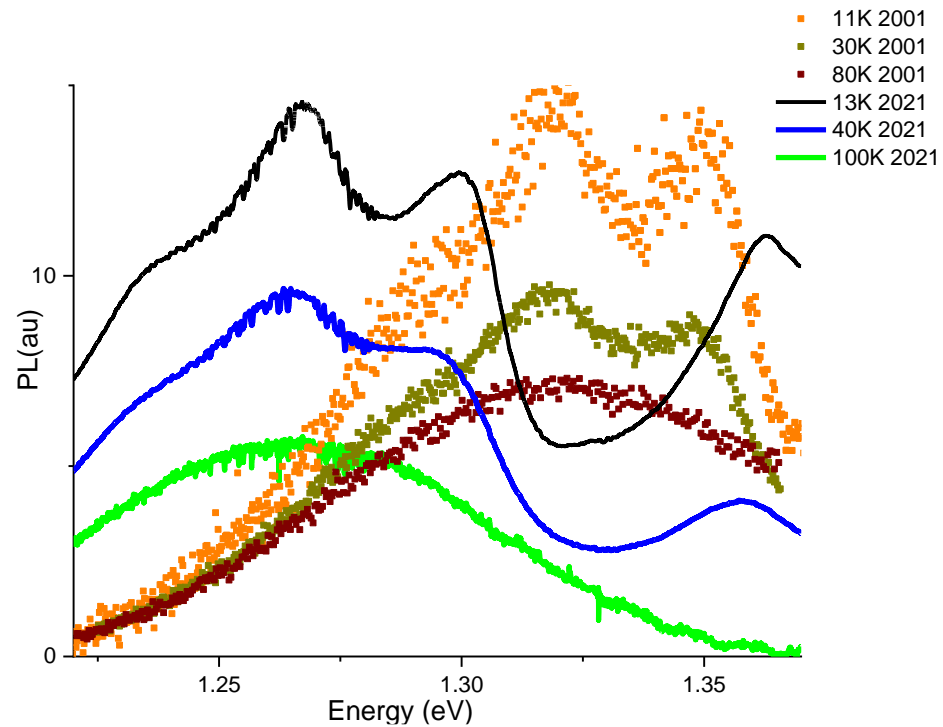


Figure 3. Photoluminescence spectra of the defect zone for the sample GaAs:Sn 1×10^{17} cm^{-3} taken in 2001 and 2021 at different temperatures.

It is clearly seen in this figure that the spectrum of the defect zone is similar at both measurement times and that the structure is lost as the temperature increases. This similarity indicates that the type of defect is the same in 2001 and 2021. However, the spectra are shifted towards lower energies for the sample that has been aging longer. We propose a hypothesis that since the defect is of the vacancy type, what could be changing is its charge state. It is also noted in Figure 3 that the maximum of the peaks at each measurement time does not change with temperature, typical of a donor-acceptor transition which is not affected by the change in the energy gap with temperature. This donor-acceptor pair must be between an impurity and the As vacancy, which forms a complex $I-V_{As}$ as reported by several authors [15,16]. In addition, it can be seen that at temperatures below 40 K, the defect peaks have a structure made up of two peaks and a shoulder, separated by 0.030 eV corresponding to the LO phonon of GaAs [15].

PR is a surface-modulated optical technique that has been mostly used to measure the critical points of the solid, in particular the energy gap. In this technique, the change in reflectance over reflectance at a specific wavelength is measured. As it is a superficial technique, these changes are proportional to the ability of the electric field of light to affect the surface charges of the material. Figure 4 shows the PR spectra taken in 1995, 2001 and 2021 for a GaAs:Sn 1×10^{17} atoms cm^{-3} sample. The spectra were fitted using a line composed of the combination of a first derivative Lorentzian function (FDLF) (for the

exciton) and a third derivative Lorentzian function (TDFL) (for the band-to-band transition), which is known as the Aspnes equation [20]:

$$\frac{\Delta R}{R} = \text{Re}\left(\sum_{j=1}^n C_j e^{i\theta_j} (\hbar\omega - E_j + i\Gamma_j)^{-m}\right) \quad (1)$$

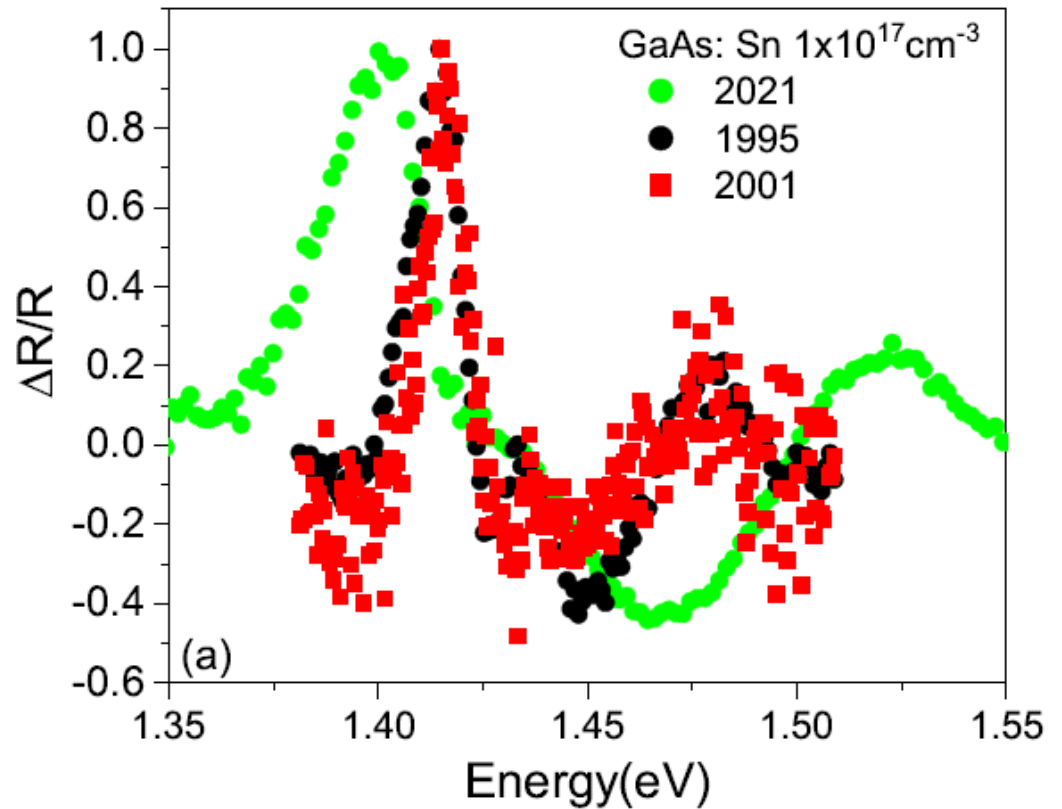


Figure 4. PR spectrum taken for the GaAs:Sn $1 \times 10^{17} \text{ cm}^{-3}$ sample at 300 K on different dates.

In Equation (1), the parameter m takes the value of 2.5 for the band-to-band transition and 2 for the excitonic transition. Four fitting parameters are used in the line shape analysis: C_j , θ_j , E_j and Γ_j . C_j is the amplitude of the shape of the j line, θ_j the phase angle, Γ_j the phenomenological broadening parameter and E_j the energy of the j th transition. The letter j runs for 2 values of transitions, the excitonic and the band-to-band. The results of these fittings are listed in Table 1 for the results of 2001 and 2021.

Table 1. Results of fitting to the PR spectra with Equation (1).

	2021				2001			
	1×10^{16}	1×10^{17}	2×10^{18}	1×10^{19}	1×10^{16}	1×10^{17}	2×10^{18}	1×10^{19}
N (atoms cm^{-3})	1×10^{16}	1×10^{17}	2×10^{18}	1×10^{19}	1×10^{16}	1×10^{17}	2×10^{18}	1×10^{19}
C_1	3.16	5.44	1.41	3.22	2.18	4.31	16.11	4.20
E_g (eV)	1.4164	1.4142	1.4055	1.4031	1.4196	1.4174	1.4070	1.4050
Γ_1 (eV)	0.025	0.049	0.420	0.512	0.014	0.024	0.100	0.250
θ_1	−2.760	0.584	0.965	0.788	−2.156	0.088	3.124	−0.005
C_2	9.15	8.32	4.39	7.16	8.16	10.12	32.11	15.92
E_x (eV)	1.4096	1.4068	1.3988	1.3961	1.4123	1.4107	1.3997	1.3977
Γ_2 (eV)	0.049	0.032	0.081	0.193	0.005	0.019	0.074	0.120
θ_2	−12.570	−1.483	−1.506	−6.209	0.052	0.092	0.433	−0.051

The undoped GaAs sample did not give an observable PR signal in 2001 and 2021. For this sample, no change in reflectance could be measured, possibly because the electric field of the exciting light turned out to be very small in the face of the high surface electric field of the charged vacancies. The impossibility of obtaining a PR spectrum in the undoped sample shows the low crystalline quality of the aged undoped GaAs sample, as mentioned above. With this analysis, it was found that the exciton energy, $E_{ex} = E_x - E_g$, gave an average of 7.3 meV in correspondence with the reported value of 7.2 meV [15]. The linewidth of both the exciton and the band-to-band transition increased considerably with aging.

Table 1 shows the values of E_g obtained from fitting Equation (1) to the PR spectra for the different concentrations of impurities in the GaAs samples. With the E_g values and the concentrations of the impurities, we draw the red dots in Figure 5. The fitted values are shown in Figure 5 (red points and line). The theoretical energy gap values based on the concentration given by Equation (2) [21] are plotted in black.

$$E_{g\ 300K} = 1.424\text{ eV} - aN^{1/3} \quad (2)$$

where N is the impurity concentration and $a = 9.8 \times 10^{-9}$ eVcm for p-type GaAs and $a = 16.5 \times 10^{-9}$ eVcm for n-type GaAs. In our case, doping with Sn generated an n-type semiconductor and a p-type semiconductor with Ge. As observed in Figure 5, the value of E_g obtained from PR exhibits a larger shift compared to the calculated value. This is because Equation (1) does not include the defects formed in GaAs over the 26 years. To incorporate the defects, the value of N in Equation (2) was changed to $N + x$, and x was solved for the different experimental values of E_g . This yielded an average value of x or defect concentration of 5×10^{17} atoms cm^{-3} . When we add this concentration of defects to N of Equation (1), the agreement is quite good. This value of the vacancy concentration is in line with the value obtained in another publication of ours using Raman spectroscopy [19], which indicates a value of 7×10^{17} cm^{-3} .

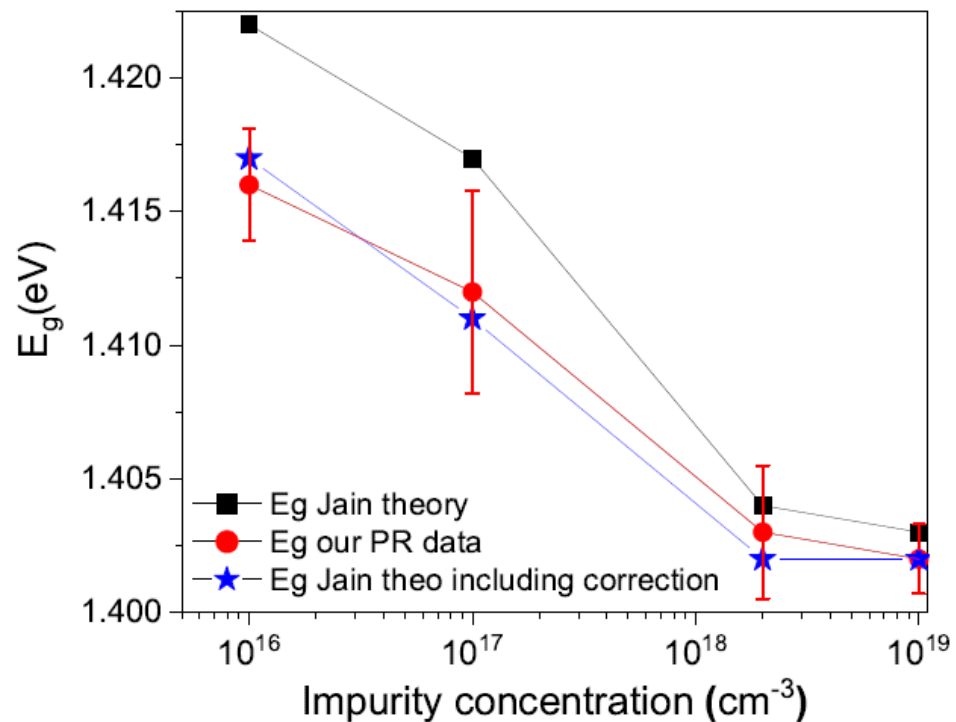


Figure 5. Values of the energy gap in GaAs according to Equation (1) and the energy gap values obtained from the PR fitting (shown in red). The stars include the correction explained in the main text.

We reviewed the phenomenological broadening parameter in Table 1 because we can obtain information about the energy depth of the deep traps or defects. The total width squared is the sum of the squares of the instrumental, phononic or thermal, defects and impurities contributions, as follows:

$$\Gamma_{obs}^2 = \Gamma_{int}^2 + \Gamma_{pho}^2 + \Gamma_{def}^2 + \Gamma_{imp}^2 \quad (3)$$

For the width of defects, we will use the expression proposed by Zdansky and Hawkins [22]

$$\Gamma_{def} = (\Gamma_{tr}(N_T + 1)p)(\exp(-2N_T S)) \quad (4)$$

In Equation (4), Γ_{tr} is the internal width of the trap, N_T is the thermal distribution of the phonons, S is the Huang-Rhys factor or average of participating phonons and p is the ratio of the trap energy to the phonon energy. We already saw previously that the participating phonon is the LO phonon and that there are two phonons participating in the spectra in Figure 3, and therefore, $S = 2$. Calculation of the thermal distribution of the LO phonon at 300 K gives 0.46. In this way, Equation (4) becomes:

$$\Gamma_{def} = (\Gamma_{tr}(1.46)^p)(0.025). \quad (5)$$

From here we will do a rough calculation to estimate the value of the trap's energy. We took the observed PR widths from Equation (3) in 2021 (Γ_{21}^2) and 2001 (Γ_{01}^2) and subtract them. In this way, the instrumental width and the phononic width cancel out and we will assume that the width of the trap is the same since we have argued that the defect is the same only when its charge state changes. We will also consider that in low doping, the width due to impurities is negligible compared to the width of the defects. In this way, the calculations are:

$$\Gamma_{21}^2 - \Gamma_{01}^2 = \Gamma_{tr}^2 [1.46^{2p_{21}} - 1.46^{2p_{01}}] \quad (6)$$

Fonthal [14] measured $p_{01} = 3$ and $\Gamma_{tr} = 0.007$ eV in 2001. From Table 1, we take the widths Γ_{21} and Γ_{01} equivalent to Γ_1 for the 1×10^{16} cm⁻³ sample in 2021 and 2001, respectively. That way, p_{21} will be 4.74. Since the energy of the trap is $E_t = 0.030p$ eV, then $E_{t01} = 0.090$ eV and $E_{t21} = 0.142$ eV.

Xu and Lindefelt [23] calculated the different charge states in both V_{Ga} and V_{As} . They obtained the following values for the V_{Ga} in its different states of charge: 0.100 eV for charge (-1), 0.068 eV for charge (-2) and 0.051 eV for charge (-3). On the other hand, for V_{As} they obtained the values: 0.145 eV for charge (-1), 0.088 eV for charge (-2) and 0.042 eV for charge (-3). The approximate calculation carried out with Equation (6) yielded values very similar to those reported by Xu and Lindefelt, in particular for the charge (-2) and (-1) of the As vacancy, which is the vacancy that has the highest probability to be formed, because the films grew rich in Ga. An inspection of the position of the maximum peaks in the spectra of Figure 3 gives a difference of 0.052 eV, very close to the difference between the As vacancy energy in the charge state (-2) and the state (-1). Furthermore, the DT, DF and DO peaks in Figure 1 are located at 0.066 eV, 0.101 eV and 0.180 eV, respectively, with respect to the energy gap of GaAs at 300 K (1.424 eV). These values do not give as close results as the previous ones when compared to the charge states of the deep trap energy level of the As vacancy. However, if we subtract the LO phonon energy (0.030 eV) for GaAs from each one, the values we obtain are 0.036 eV, 0.071 eV and 0.150 eV, which are quite close to the trap energies for the charge values (-3), (-2) and (-1) for the As vacancy. Subtracting the phonon LO is justified because vacancies deform the lattice in what is called the Sach-Teller deformation, and therefore, an electron that transits from the conduction band to the vacancy level loses thermal energy due to the rearrangement of the lattice.

It can be stated that the aging process of our GaAs samples is due to the oxygen in the air that produces vacancies due to the oxidation of Ga and mainly As. These vacancies begin in a charge state of (-3) over the years, and they change their state of charge up to (-1) by

self-compensation. The aging effect is mainly manifested in the undoped samples, whereas in the doped samples, the impurities Ge and Sn prevent the formation of As vacancies since these impurities occupy Ga and As sites because these elements are amphoteric.

4. Conclusions

The analysis of PL at various temperatures and PR at 300 K in Ge and Sn-doped and undoped GaAs epitaxial films over three periods since 1995 allowed us to observe the aging dynamics of samples stored in a dark and dry environment. We found that aging created defects mainly in vacancy type, which resulted in deep trap energy levels and concentrations of 5×10^{17} atoms cm^{-3} . The impurification through substitutional impurities decreases the deterioration of the sample as Ge and Sn replace Ga and As atoms, preventing the formation of deep traps as vacancies of these last two elements. We were able to estimate the defect trap energies and found that they corresponded to the energies assigned to the charge states (−2) and (−1) of the As vacancy for PR results in 2001 and 2021. There is a dynamic of slow changes in semiconductor materials that age the material over time and affect its photo-response. We recommend both manufacturers and materials researchers store semiconductor samples in an oxygen-free environment to delay the aging process.

Author Contributions: S.Z.R.: experimental measurements, formal analysis, writing of the manuscript, and original draft preparation; G.F.: conceptualization, methodology, supervision, formal analysis, writing of the manuscript. All authors have read and agreed to the published version of the manuscript.

Funding: We are grateful to the Instituto Interdisciplinario de las Ciencias, Universidad del Quindío for the use of their facility and the Universidad de la Guajira for support through Vicerrectoria de Investigacion.

Institutional Review Board Statement: Not applicable.

Informed Consent Statement: Not applicable.

Data Availability Statement: No new data were created or analyzed in this study. Data sharing is not applicable to this article.

Conflicts of Interest: The authors declare no conflict of interest.

References

1. Yang, C.; Zhan, S.; Li, Q.; Wu, Y.; Jia, X.; Li, C.; Liu, K.; Qu, S.; Wang, Z. Systematic investigation on stability influence factors for organic solar cells. *Nano Energy* **2022**, *98*, 107299. [[CrossRef](#)]
2. Khan, S.; Agbo, I.; Hamdouil, S.; Kukner, H.; Kaczer, B.; Raghavan, P.; Catthoor, F. Bias temperature instability analysis of FinFET based SRAM cells. In Proceedings of the 2014 Design, Automation & Test in Europe Conference & Exhibition (DATE), Dresden, Germany, 24–28 March 2014; Volume 31.
3. Quesnel, E.; Poncet, S.; Altazin, S.; Lin, Y.P.; D’Amico, M. Lifetime prediction of encapsulated CdSexS1-x quantum platelets for color conversion in high luminance LED microdisplays. *Opt. Express* **2023**, *31*, 10955–10964. [[CrossRef](#)] [[PubMed](#)]
4. Shimamura, K.; Takehara, T.; Ikeda, N. Measurement Results of Real Circuit Delay Degradation under Realistic Workload. *IPSI Trans. Syst. LSI Des. Methodol.* **2023**, *16*, 27–34. [[CrossRef](#)]
5. Yang, B.; Mei, S.; Zhu, Y.; Yang, D.; He, H.; Hu, R.; Li, Y.; Zou, J.; Guo, R. Precipitation promotion of highly emissive and stable CsPbX₃ (Cl, Br, I) perovskite quantum dots in borosilicate glass with alkaline earth modification. *Ceram. Int.* **2023**, *49*, 6720–6728. [[CrossRef](#)]
6. Kim, H.-M.; KIM, D.-G.; Kim, Y.-S.; Kim, M.; Park, J.-S. Atomic layer deposition for nanoscale. *Int. J. Extrem. Manuf.* **2023**, *5*, 012006. [[CrossRef](#)]
7. Kumara, D.; Shinga, A.; Shindeb, V.; Kura, R. Sol-Ageing Effect on the Structural and Optical Properties of Undoped and Doped ZrO₂ Thin Films. *Prot. Met. Phys. Chem. Surf.* **2022**, *58*, 999–1010. [[CrossRef](#)]
8. Song, Y.; Lv, Z.; Niu, S.; Wu, Z.; Qin, L.; Chen, Y.; Liang, L.; Lei, Y.; Jia, P.; Shan, X.; et al. Processes of the Reliability and Degradation Mechanism of High-Power Semiconductor lasers. *Crystals* **2022**, *12*, 765. [[CrossRef](#)]
9. Rajput, N.S.; Kotbi, A.; Kaja, K.; Jouiad, M. Long-term aging of CVD grown 2D-MoS₂ nanosheets in ambient environment. *Mater. Degrad.* **2022**, *6*, 75. [[CrossRef](#)]

10. Yoon, S.; Seo, M.; Kim, I.S.; Kwangyeol, L.; Woo, K. Woo Ultra-Stable and Highly Efficient White Light Emitting Diodes through CsPbBr₃ Perovskite nanocrystals Silica Composite Phosphor Functionalized with Surface Phenyl Molecules. *Small* **2023**, *19*, 2206311. [[CrossRef](#)]
11. Yang, X.; Sang, Q.; Zhang, J.; Wang, C.; Yu, M.; Zhao, Y. A high-efficiency aging test with new data processing method for semiconductor device. *Microelectron. Reliab.* **2023**, *143*, 114940. [[CrossRef](#)]
12. Neuhold, I.; Noga, P.; Sojak, S.; Petriska, M.; Degmova, J.; Slugen, V.; Krsjak, V. Application of Proton Irradiation in the Study of Accelerated Radiation Ageing in a GaAs semiconductor. *Materials* **2023**, *16*, 1089. [[CrossRef](#)] [[PubMed](#)]
13. Torres-Delgado, G.; Mendoza-Alvarez, J.G.; Vasquez-López, C.; Alejo-Armenta, C. Photoluminescence and photorefectance studies of defects in GaAs epitaxial layers grown by liquid phase epitaxy at different supercooling temperatures. *J. Vac. Sci. Technol. A Vac. Surf. Film.* **1997**, *15*, 971–975. [[CrossRef](#)]
14. Fonthal, G. *Estudio de la Impurificación de Capas Epitaxiales de GaAs y AlGaAs en el Rango de Leve Hasta Fuerte Dopaje por Medio de Fotoluminiscencia y Fotorreflectancia*; Universidad del valle: Cali, CO, USA, 2001.
15. Pavezzi, L.; Guzzi, M. Photoluminescence of Al_xGa_{1-x}As alloys. *J. Appl. Phys.* **1994**, *75*, 4779. [[CrossRef](#)]
16. Sermage, B.; Long, S.; Deveaud, B.; Katzer, D. Lifetime of excitons in GaAs quantum well. *J. Phys. IV Proc.* **1993**, *C5*, 19–25.
17. Birey, H.; Sites, J. Radiative transitions induced in gallium arsenide by modest heat treatment. *J. Appl. Phys.* **1980**, *51*, 619. [[CrossRef](#)]
18. Bunea, M.M.; Dunham, S.T. Monte Carlo study of vacancy mediated impurity diffusion in silicon. *Phys. Rev. B* **2000**, *61*, 2397. [[CrossRef](#)]
19. Zambrano, S.; Fonthal, G.; Salas, G.E.E.; Ortega, J.S. Formation of point defects due to aging under natural conditions of doped GaAs. *Materials* **2023**.
20. Kopaczek, J.; Dybala, F.; Zelewski, S.J.; Sokolowski, N.; Zuraw, W.; McNicholas, K.M.; El-Jarouidi, R.H.; White, R.C.; Bank, S.R.; Kudrawier, R. Photorefectance studies of temperature and hydrostatic pressure dependencies of direct optical transitions in BGaAs alloys grown on GaP. *J. Phys. D Appl. Phys.* **2022**, *55*, 015107. [[CrossRef](#)]
21. Jain, C.; Mcgregor, J.M.; Roulston, D.I. Band-gap narrowing in novel III-V semiconductors. *J. Appl. Phys.* **1990**, *68*, 3747. [[CrossRef](#)]
22. Zdansky, K.; Hawkins, I.D. Slow decay of photoconductivity caused by tin-related DX centers in AlGaAs. *Czechoslov. J. Phys.* **1999**, *49*, 813. [[CrossRef](#)]
23. Xu, H.; Lindefelt, U. Electronic structure of neutral and charged vacancies in GaAs. *Phys. Rev. B* **1990**, *41*, 5976–5990. [[CrossRef](#)] [[PubMed](#)]

Disclaimer/Publisher’s Note: The statements, opinions and data contained in all publications are solely those of the individual author(s) and contributor(s) and not of MDPI and/or the editor(s). MDPI and/or the editor(s) disclaim responsibility for any injury to people or property resulting from any ideas, methods, instructions or products referred to in the content.